



## BIROn - Birkbeck Institutional Research Online

Crawford, Ian (1992) High-resolution observations of the interstellar NaI UV doublet and a discussion of the resulting NaI/CaII ratios. *Monthly Notices of the Royal Astronomical Society* 259 (1), pp. 47-62. ISSN 0035-8711.

Downloaded from: <https://eprints.bbk.ac.uk/id/eprint/28633/>

*Usage Guidelines:*

Please refer to usage guidelines at <https://eprints.bbk.ac.uk/policies.html>  
contact [lib-eprints@bbk.ac.uk](mailto:lib-eprints@bbk.ac.uk).

or alternatively

# High-resolution observations of the interstellar $\lambda 3302$ Na I doublet and a discussion of the resulting Na I/Ca II ratios

I. A. Crawford

Department of Physics and Astronomy, University College London, Gower Street, London WC1E 6BT

Accepted 1992 April 28. Received 1992 April 14; in original form 1992 January 28

## SUMMARY

High-resolution ( $6 \text{ km s}^{-1}$  FWHM) observations of the interstellar  $\lambda 3302$  Na I doublet towards 11 southern early-type stars are presented. The analysis has resulted in much more accurate Na I column densities than those obtained from earlier studies of the (fully saturated) Na *D* lines. The  $\lambda 3302$  lines have low radial velocities ( $-15 \lesssim v_{\text{lsr}} \lesssim +10 \text{ km s}^{-1}$ ) and are much simpler than the Na *D* and Ca II profiles towards the same stars, generally occurring at those velocities previously identified with diffuse molecular clouds. Analysis of the Na I/Ca II ratios in these components indicates that  $\delta_{\text{Ca}} \approx -3$  to  $-4$  in the molecular clouds, implying that most of the Ca has been adsorbed on to the surfaces of interstellar grains. Lower Ca depletions are found in the less dense (non-molecular) clouds which are responsible for the additional absorption observed in the Na *D* and Ca *K* lines at both high and low velocities.

**Key words:** line: profiles – interstellar medium: abundances – interstellar medium: clouds – dust, extinction.

## 1 INTRODUCTION

Studies of neutral sodium in the diffuse interstellar medium have generally relied upon observations of the resonance ( $3s-3p$ ; Fraunhofer *D*) lines at 5890 and 5896 Å. However, for Na column densities greater than about  $10^{12} \text{ cm}^{-2}$  these lines begin to saturate, and column densities derived from them become very uncertain. Observations of the weaker ( $3s-4p$ ) doublet at 3302 Å have the potential to resolve this difficulty because, with oscillator strengths only 1.4 per cent of those of the *D* lines (Morton 1991), significant saturation does not occur until the column density is some two orders of magnitude higher.

Here we report observations of the  $\lambda 3302$  Na doublet towards 11 southern stars. As we are also interested in the Na I/Ca II ratios, the Ca II *K* line was observed towards three stars for which observations have not been obtained previously with the same instrument. Basic observational data for the stars observed are given in Table 1.

## 2 OBSERVATIONS

The observations were obtained with the coude echelle spectrograph of the Mt Stromlo 74-inch telescope in 1991 June and July. The spectrograph was used with the 130-inch focal length camera, giving a dispersion of  $0.29 \text{ Å mm}^{-1}$  at the  $\lambda 3302$  Na I doublet, and  $0.35 \text{ Å mm}^{-1}$  at the Ca II *K* line. The slit widths were  $500 \mu\text{m}$  for the Na lines (corresponding to a velocity resolution of  $6 \text{ km s}^{-1}$  FWHM) and  $250 \mu\text{m}$  ( $3 \text{ km s}^{-1}$ ) for the Ca lines (a wider slit was adopted for the Na doublet owing to the lower efficiency of the system at the shorter wavelength). The detector was the Mt Stromlo Photon Counting Array (PCA; Rodgers *et al.* 1988); exposure times are given in Table 1.

The spectra were extracted from the PCA image using the FIGARO package (Shortridge 1988) on the University College London STARLINK node. The inter-order background, obtained from PCA rows on either side of the spectrum, was subtracted; previous work with this spectrograph (e.g. Crawford, Barlow & Blades 1989) has indicated that the resulting zero intensity level may be uncertain by up to 4 per cent of the continuum intensity. The spectra were divided by a flat-field, wavelength-calibrated by means of a Th–Ar lamp, and converted to the LSR velocity frame. Finally, as the 130-inch camera yields 15 PCA pixels across the  $6 \text{ km s}^{-1}$  FWHM instrumental response function, the  $\lambda 3302$  spectra were rebinned so as to reduce this to five; this procedure has greatly improved the signal-to-noise ratio of the final spectra, but has not degraded the resolution (indeed, by conventional standards, the instrumental response function remains oversampled).

**Table 1.** Basic observational data and exposure times for the stars observed. The quantity  $\Delta v_{\text{lsr, hel}}$  should be subtracted from the LSR velocities used throughout this paper in order to recover the heliocentric values.

HD	Name	<i>V</i>	<i>E</i> ( <i>B</i> − <i>V</i> )	Ref.	Spectral Type	Ref.	<i>l</i> (°)	<i>b</i> (°)	Dist. (pc)	Ref.	Exp. Na I (hr)	Exp. Ca II (hr)	$\Delta v_{\text{lsr, hel}}$ (km s <sup>−1</sup> )
110432	....	5.3	0.40	1	B0.5 IIIe	1	302.0	−0.2	430	1	3.0	...	−7.6
142114	2 Sco	4.6	0.11	2	B2.5 V	2	346.9	+21.6	112	2	2.5	...	+8.6
144470	$\omega^1$ Sco	4.0	0.22	2	B1 V	2	352.8	+22.8	183	2	2.8	...	+10.3
148184	$\chi$ Oph	4.4	0.57	2	B2 IVpe	2	357.9	+20.7	263	2	3.0	...	+11.5
149038	$\mu$ Nor	4.9	0.31	3	O9.7 Iab	3	339.4	+2.5	960	3	2.0	1.0	+4.4
149757	$\zeta$ Oph	2.6	0.28	2	O9 V	3	6.3	+23.6	228	2	1.4	0.7	+13.7
151804	....	5.2	0.35	4	O8 Iaf	3	343.6	+1.9	1900	4	3.1	...	+5.6
152236	$\zeta^1$ Sco	4.7	0.69	4	B1.5 Ia <sup>+</sup>	3	343.0	+0.9	1900	4	3.6	...	+5.3
152249	....	6.5	0.48	4	OC9.5 Iab	3	343.5	+1.2	1900	4	4.0	...	+5.5
152270	....	6.6	0.48	4	WC7+O5	2	343.5	+1.2	1900	4	6.6	...	+5.5
154368	....	6.1	0.78	3	O9.5 Iab	3	350.0	+3.2	860	3	3.5	2.0	+7.7

References to colour excesses: (1) Codina *et al.* (1984); (2) calculated from the spectral type, assuming the intrinsic colours of Deutschman, Davis & Schild (1976) and the observed colours given by Schild, Garrison & Hiltner (1983; HD 154368) and Hoffleit & Jaschek (1982; HD 149038); (4) van Genderen, Bijleveld & van Groningen (1984). References to spectral types: (1) Codina *et al.* (1984); (2) Hoffleit & Jaschek (1982); (3) listed by Prinja, Barlow & Howarth (1990). References to distances: (1) Codina *et al.* (1984); (2) de Geus *et al.* (1989); (3) Calculated from the spectral types and absolute magnitudes of Deutschman *et al.* (1976); (4) OB association distance (Humphreys 1978).

The spectra of the  $\lambda$ 3302 Na I doublet for all 11 stars are shown in Fig. 1, and the new Ca II spectra obtained for three of these stars are shown in Fig. 2. In addition, Fig. 2(b) shows a previously unpublished spectrum of the interstellar Na I  $D_2$  line toward  $\zeta$  Oph (obtained by Drs M. J. Barlow and J. C. Blades in 1979; personal communication), which may be used to compare the Na *D* and  $\lambda$ 3302 results for this star (see also Hobbs 1969a, 1978).

### 3 EQUIVALENT WIDTHS, LINE PROFILES AND COLUMN DENSITIES

Equivalent widths and radial velocities were measured by fitting Gaussians to the observed line profiles (using DIPSO; Howarth & Murray 1988). In the case of the  $\lambda$ 3302 doublet, both components were fitted simultaneously, but constrained to have identical FWHM and to be separated by the known separation of the doublet (0.610 Å; Morton 1991). The resulting values are given in Tables 2 and 3 for the Na I  $\lambda$ 3302 and Ca II *K* lines respectively; the quoted errors are  $1\sigma$  values and, in the case of the equivalent widths, include an assumed 4 per cent zero-level error. It was found that, for stars with multiple velocity components, the sum of the equivalent widths obtained from the least-square Gaussian fits (Table 2) lies within the  $1\sigma$  errors of the total equivalent widths measured directly from the observed line profiles.

#### 3.1 Na I column density analysis

The two components of the  $3s$ – $4p$  Na I doublet have wavelengths of 3302.368 and 3302.978 Å, with oscillator strengths of  $8.97 \times 10^{-3}$  and  $4.48 \times 10^{-3}$ , respectively (Morton 1991). However, each of these is itself an unresolved doublet owing to hyperfine splitting in the Na I ground state (*cf.* the energy level diagram given by McNutt & Mack 1963), and the measured equivalent widths are due to a blend of the two hyperfine components. These components have relative strengths in the ratio of the statistical weights ( $2F+1$ ) of the hyperfine levels; i.e., in this case,  $5/8$  and  $3/8$  of the total oscillator strengths given by Morton (1991). This structure has been directly observed in very high-resolution studies of the interstellar Na *D* lines (e.g. Hobbs & Welty 1991, and references therein).

Expressed in velocity units, the hyperfine splitting amounts to  $0.6 \text{ km s}^{-1}$  at a wavelength of 3302 Å; this is comparable to the intrinsic velocity dispersions (*b* values) of lines formed in diffuse interstellar clouds, and must therefore be allowed for in the analysis. Hobbs (1969b) has given an expression for the absorption coefficient which takes into account the effect of hyperfine splitting (his equation 3). Adopting Hobbs' notation, we have an expression for the equivalent width,  $w_\lambda$ , resulting from a blend of the two hyperfine components:

$$\frac{w_\lambda}{b_\lambda} = \int_{-\infty}^{+\infty} \left[ 1 - \exp \left\{ -\frac{3}{8} \tau_0 \exp \left[ -\left( x + \frac{\alpha}{2} \right)^2 \right] - \frac{5}{8} \tau_0 \exp \left[ -\left( x - \frac{\alpha}{2} \right)^2 \right] \right\} \right] dx, \quad (1)$$

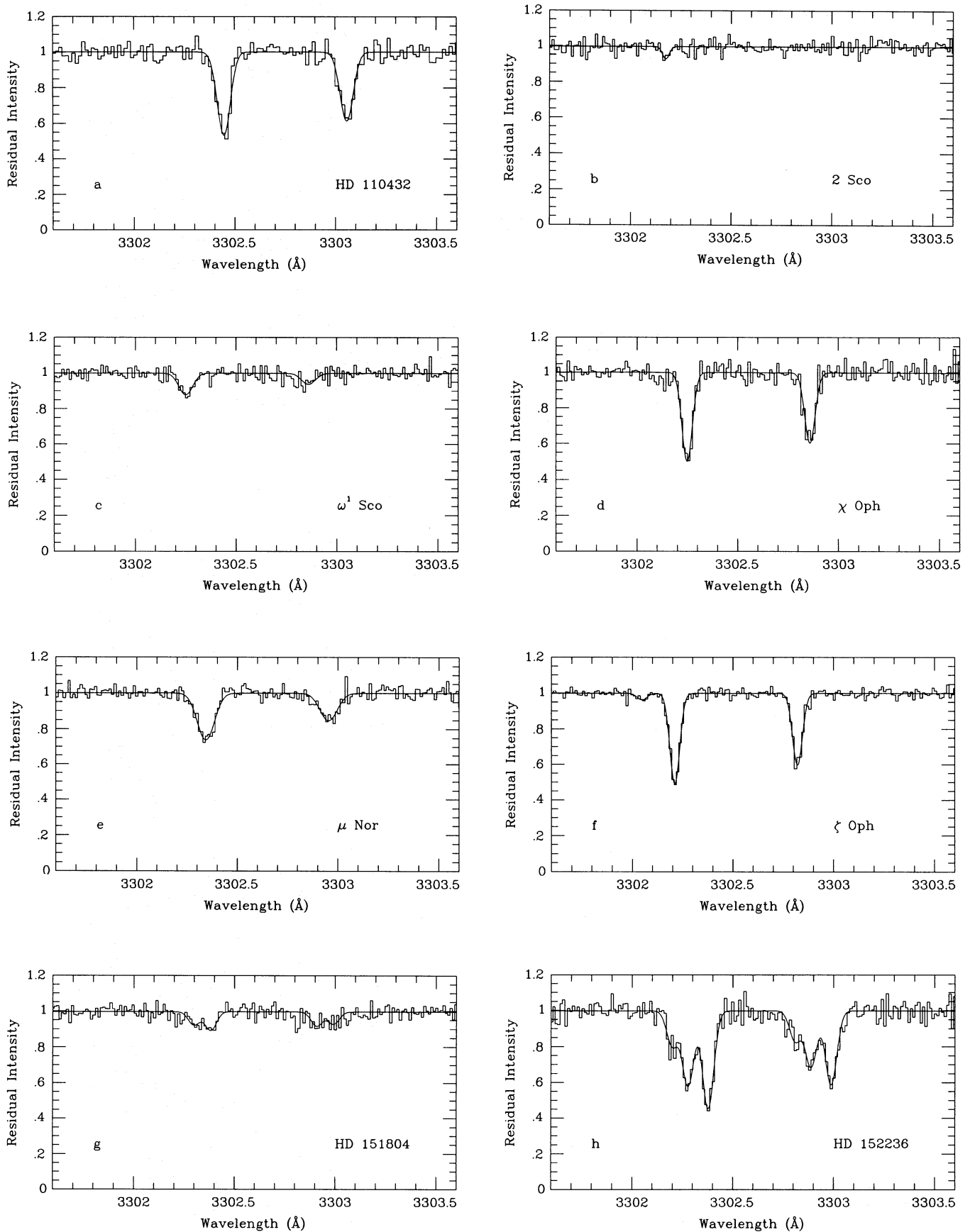


**Figure 1.** The interstellar  $\lambda 3302$  Na I doublet observed towards all 11 stars. The observed spectra are plotted as histograms; the smooth curves are the least-square Gaussian fits which yielded the velocities and equivalent widths given in Table 2. The wavelength scale is heliocentric.

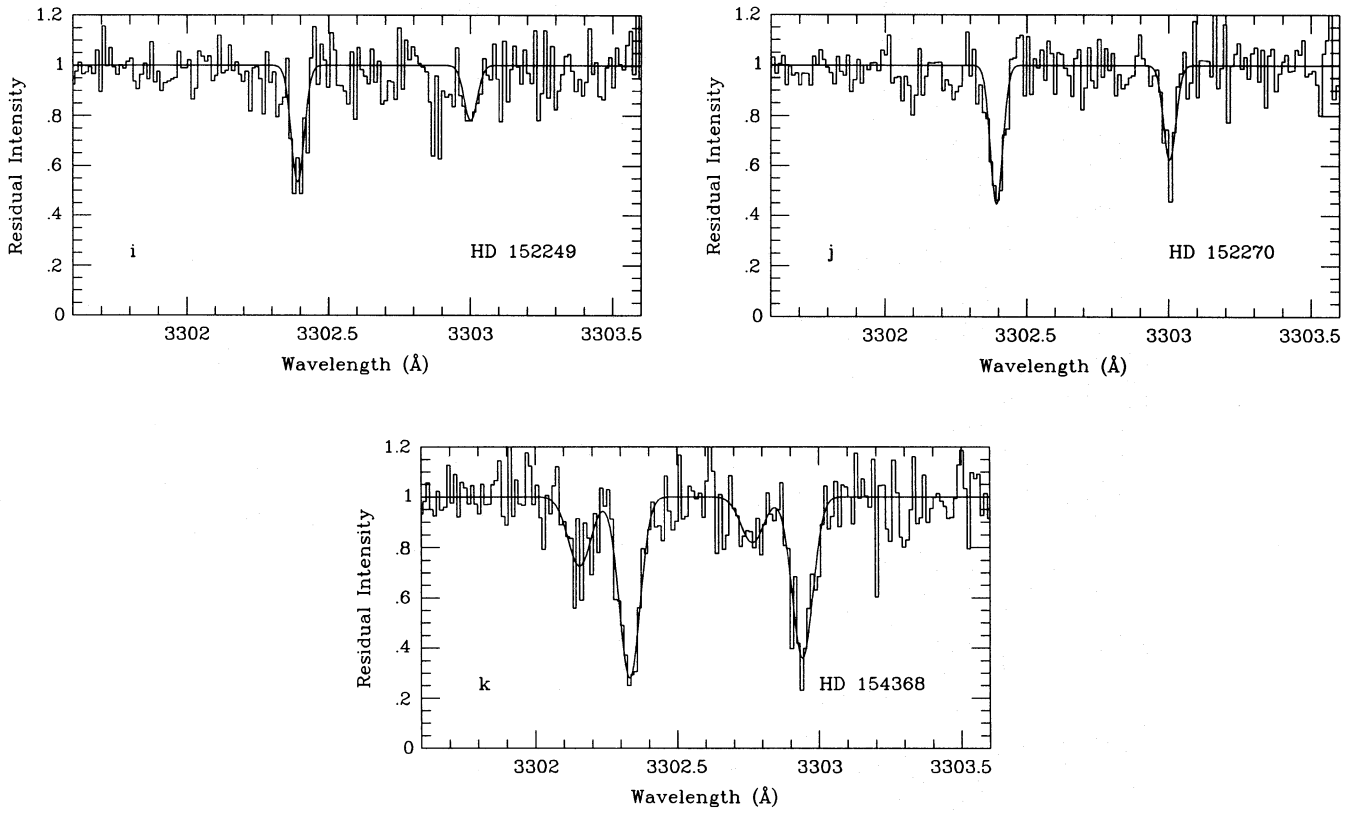


Figure 1 - continued

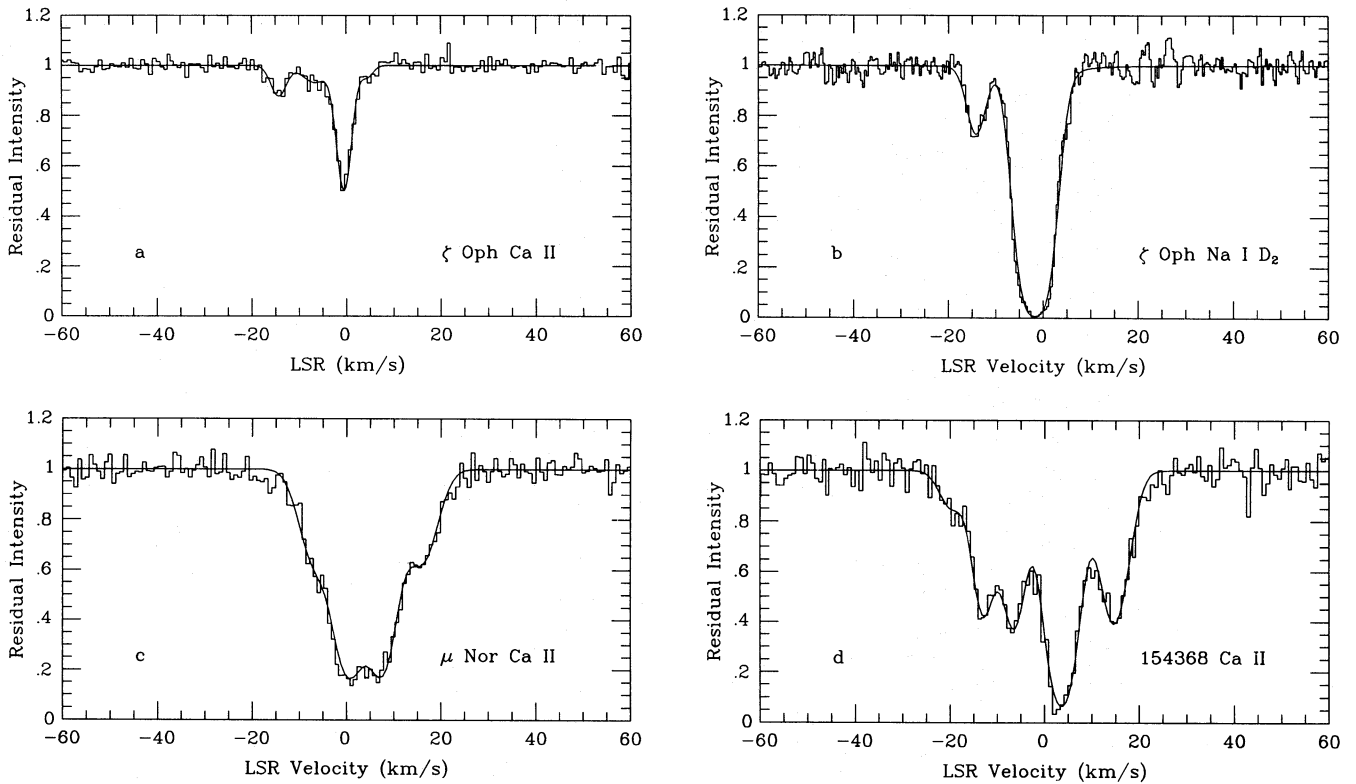


Figure 2. The interstellar Ca II lines observed towards  $\zeta$  Oph,  $\mu$  Nor and HD 154368, plus a spectrum (b) of the Na I  $D_2$  line towards  $\zeta$  Oph (Drs M. J. Barlow & J. C. Blades, personal communication). The observed spectra are plotted as histograms; the smooth curves are model line profiles with the parameters given in Table 3.

**Table 2.** LSR velocities, equivalent widths, velocity dispersions and column densities obtained from the analysis of the  $\lambda$  3302 Na I doublet.

Star	$v_{\text{LSR}}$ (km s <sup>-1</sup> )	$w_{\lambda}(3302)$ (mÅ)	$w_{\lambda}(3303)$ (mÅ)	$b$ (km s <sup>-1</sup> )	Log $N$ (cm <sup>-2</sup> )	Notes
110432	$-0.5 \pm 0.1$	$38.3 \pm 2.8$	$31.7 \pm 2.8$	$1.0^{+0.4}_{-0.24}$	$14.30^{+1.16}_{-0.24}$	
2 Sco	$-9.0 \pm 0.7$	$2.9 \pm 1.0$	$\leq 1.5$	$\leq 3.6$	$12.54^{+0.34}_{-0.18}$	1,2
$\omega^1$ Sco	$-0.4 \pm 0.4$	$10.3 \pm 1.5$	$5.2 \pm 1.4$	$3.8^{+1.2}_{-3.6}$	$13.10^{+0.26}_{-0.06}$	1
$\chi$ Oph	$+0.6 \pm 0.1$	$32.6 \pm 2.0$	$25.9 \pm 1.9$	$0.9^{+0.3}_{-0.2}$	$14.12^{+0.30}_{-0.16}$	
$\mu$ Nor	$+2.1 \pm 0.2$	$28.0 \pm 1.8$	$16.3 \pm 1.8$	$2.1^{+3.9}_{-1.0}$	$13.64^{+0.12}_{-0.08}$	1
$\zeta$ Oph	$-15.4 \pm 1.0$	$2.2 \pm 0.7$	$\leq 1.0$	$\leq 3.6$	$12.42^{+0.24}_{-0.16}$	1,2
	$-0.7 \pm 0.1$	$31.2 \pm 1.3$	$24.6 \pm 1.3$	$0.9^{+0.2}_{-0.1}$	$14.08^{+0.10}_{-0.12}$	
151804	$-0.8 \pm 0.7$	$5.2 \pm 1.2$	$5.5 \pm 1.1$	$\leq 0.1$	$13.35^{+0.05}_{-0.05}$	2,3
	$+6.7 \pm 0.5$	$7.2 \pm 1.2$	$4.7 \pm 1.1$	$0.3^{+3.3}_{-0.2}$	$13.10^{+0.46}_{-0.16}$	1
152236	$-10.1 \pm 0.6$	$13.7 \pm 2.9$	$11.8 \pm 2.7$	$\leq 1.5$	$\geq 13.38$	4
	$-3.0 \pm 0.3$	$29.5 \pm 4.2$	$22.0 \pm 3.6$	$0.9^{+2.5}_{-0.5}$	$13.96^{+1.40}_{-0.28}$	
	$+6.1 \pm 0.2$	$38.2 \pm 3.4$	$28.9 \pm 3.1$	$1.2^{+0.8}_{-0.5}$	$14.10^{+0.68}_{-0.20}$	
152249	$+7.5 \pm 0.3$	$26.8 \pm 3.5$	$12.7 \pm 3.2$	$2.7^{+0.9}_{-1.8}$	$13.56^{+0.16}_{-0.06}$	1
152270	$+7.7 \pm 0.2$	$30.2 \pm 3.5$	$20.5 \pm 3.1$	$1.2^{+2.4}_{-0.6}$	$13.84^{+0.44}_{-0.18}$	1,5
154368	$-11.7 \pm 0.7$	$27.6 \pm 5.5$	$18.3 \pm 5.3$	$1.1^{+4.9}_{-0.7}$	$13.78^{+1.20}_{-0.28}$	1
	$+4.3 \pm 0.2$	$65.1 \pm 5.7$	$57.8 \pm 5.6$	$\leq 2.4$	$\geq 14.34$	4

Notes: (1) Upper limit to  $b$  (and hence lower limit to  $N$ ) constrained by the observed width of the absorption-line profile. (2) Upper limit to  $N$  obtained by assuming a lower limit to  $b$  of 0.1 km s<sup>-1</sup>, corresponding (in the absence of turbulence) to a kinetic temperature of 14 K; see text. (3) The very low  $b$  value results from the fact that both components of the doublet appear to have approximately equal strength; however, note the poor signal-to-noise ratio in the vicinity of the  $\lambda$  3303 line. (4) Owing to the low doublet ratios, it was not possible to obtain reliable column density upper limits for these components. However, the observations of the Na I  $D_2$  lines (Crawford *et al.* 1989) indicate an upper limit of  $\log N \sim 15$  (implying  $b \geq 0.2$  and  $\geq 1.3$  km s<sup>-1</sup> for the indicated components towards HD 152236 and 154368, respectively). (5) Owing to the failure to record a comparison spectrum for this star, the velocity has been set to that of the single CH line observed towards this star by Crawford (1989); see text.

where  $b_{\lambda}$  is the velocity dispersion expressed in wavelength units (i.e.  $b_{\lambda} = b\lambda/c$ ),  $\alpha$  is the velocity separation of the two components, expressed as a fraction of the velocity dispersion (i.e. in this case,  $\alpha = 0.6$  km s<sup>-1</sup>/ $b$ ), and  $x[\equiv c(\lambda - \lambda_0)/b\lambda_0]$  is a dimensionless wavelength scale.  $\tau_0$  is given by

$$\tau_0 = Nf\lambda_0^2/2.002 \times 10^{20}b_{\lambda}, \quad (2)$$

where  $N$  is the column density (cm<sup>-2</sup>),  $f$  is the (total) oscillator strength, and  $\lambda_0$  is the rest wavelength (in Å) of the blend (*cf.* Strömgren 1948; Somerville 1988).

Equation (1) can be used to obtain the equivalent widths of each observed Na I line as a function of  $N$  and  $b$ . Conversely, since we have two such equations (one each for  $\lambda\lambda$  3302 and 3303), these may be solved simultaneously to yield  $N$  and  $b$  individually. The values obtained in this way are listed in Table 2; the uncertainties on these values were found by determining the range of  $N$  and  $b$  consistent with the observed equivalent width errors. It should be noted, however, that these values have been obtained under the assumption that the velocity components listed in Table 2 are genuinely single, and are not unresolved blends of several discrete components. If unresolved components are present within the observed line profiles, the resulting (total) column densities may have been significantly underestimated (*cf.* Nachman & Hobbs 1973).

The velocity dispersions,  $b$ , were generally found to be of the order of 1 km s<sup>-1</sup>; the three best-constrained values (i.e. for the clouds towards HD 110432,  $\chi$  Oph and the main component towards  $\zeta$  Oph) were all found to lie within a few tenths of a km s<sup>-1</sup> of this value. The velocity dispersion obtained for the  $\zeta$  Oph cloud ( $b = 0.9 \pm 0.1$  km s<sup>-1</sup>) agrees well with the range (0.7–0.9 km s<sup>-1</sup>) obtained by Morton (1975) from a curve-of-growth analysis, and is essentially identical to the very accurate value ( $0.88 \pm 0.02$  km s<sup>-1</sup>) determined by Crane *et al.* (1986) from a study of the CN lines.



**Table 3.** LSR velocities, equivalent widths, velocity dispersions and column densities obtained for the Ca II *K* line towards  $\mu$  Nor,  $\zeta$  Oph and HD 154368; these values are also given for the Na *D*<sub>2</sub> line towards  $\zeta$  Oph. Errors are  $1\sigma$  values, and allow for a possible 4 per cent zero-level error.

Star	Ion	$w_\lambda(\text{tot})$ (mÅ)	$v_{\text{lsr}}$ (km s <sup>-1</sup> )	$w_\lambda$ (mÅ)	$b$ (km s <sup>-1</sup> )	$\log N$ (cm <sup>-2</sup> )
$\mu$ Nor	Ca II	240 ± 10	-6.6 ± 0.6	36.7 ± 3.0	4.0 <sup>+1.5</sup> <sub>-1.0</sub>	11.74 <sup>+0.14</sup> <sub>-0.26</sub>
			+0.4 ± 0.2	80.2 ± 5.8	3.5 <sup>+1.0</sup> <sub>-0.5</sub>	12.26 <sup>+0.04</sup> <sub>-0.08</sub>
			+7.4 ± 0.7	78.7 ± 6.6	3.5 <sup>+1.0</sup> <sub>-0.5</sub>	12.26 <sup>+0.04</sup> <sub>-0.08</sub>
			+15.9 ± 0.9	39.7 ± 3.3	4.0 <sup>+2.0</sup> <sub>-0.5</sub>	11.74 <sup>+0.14</sup> <sub>-0.20</sub>
$\zeta$ Oph	Ca II	40 ± 2	-14.3 ± 0.3	6.6 ± 0.7	2.0 <sup>+1.0</sup> <sub>-1.0</sub>	10.90 <sup>+0.14</sup> <sub>-0.20</sub>
			-6.6 ± 0.5	4.7 ± 0.7	3.5 <sup>+1.0</sup> <sub>-0.5</sub>	10.85 <sup>+0.15</sup> <sub>-0.15</sub>
			-0.5 ± 0.2	27.8 ± 1.3	1.8 <sup>+0.4</sup> <sub>-0.3</sub>	11.59 <sup>+0.06</sup> <sub>-0.06</sub>
			+4.3 ± 0.9	2.4 ± 0.7	1.5 <sup>+1.0</sup> <sub>-0.5</sub>	10.40 <sup>+0.08</sup> <sub>-0.22</sub>
	Na I	230 ± 10	-14.3 ± 0.4	24.0 ± 2.0	≤ 1.0	11.25 <sup>+1.75</sup> <sub>-0.07</sub>
			-4.4 ± 0.3	103.0 ± 8.0	≤ 3.0	13.00 <sup>+1.30</sup> <sub>-0.70</sub>
154368	Ca II	279 ± 12	-19.7 ± 1.6	7.8 ± 3.3	3.0 <sup>+2.0</sup> <sub>-1.0</sub>	11.18 <sup>+0.12</sup> <sub>-0.18</sub>
			-13.0 ± 0.5	48.8 ± 6.3	2.5 <sup>+0.5</sup> <sub>-1.0</sub>	11.85 <sup>+0.10</sup> <sub>-0.15</sub>
			-6.5 ± 0.4	53.2 ± 6.3	2.8 <sup>+0.7</sup> <sub>-0.8</sub>	11.95 <sup>+0.09</sup> <sub>-0.10</sub>
			+3.6 ± 0.2	107.1 ± 5.9	3.5 <sup>+1.0</sup> <sub>-1.5</sub>	12.48 <sup>+0.52</sup> <sub>-0.08</sub>
			+14.7 ± 0.2	65.0 ± 5.6	3.5 <sup>+1.0</sup> <sub>-1.0</sub>	12.00 <sup>+0.11</sup> <sub>-0.10</sub>

The  $b$  values for the remaining components are less well constrained (due mainly to relatively large equivalent width errors and/or very low doublet ratios), but are all consistent with values  $\leq 1$  km s<sup>-1</sup>. For some components the  $b$  value upper limits were found to exceed those set by the observed linewidths, and in these cases (indicated in Table 2) the latter value has been adopted. In two cases it proved impossible to obtain reliable upper limits to the column density; lower limits are indicated in Table 2, but upper limits obtained from observations of the Na I *D* lines towards these stars (Crawford *et al.* 1989) are indicated in the footnotes to the table.

Finally, we note that the two weakest components in the present sample were positively identified only in the strongest line of the doublet. If only one line is available it is not possible to solve for  $N$  and  $b$  simultaneously; in Table 2 the range in  $N$  given for these components was obtained by solving equation (1) with  $b$  values between an *assumed* lower limit of 0.1 km s<sup>-1</sup> (corresponding to  $T = 14$  K, and considered to be a safe lower limit for diffuse cloud conditions), and an upper limit of 3.6 km s<sup>-1</sup> (the maximum permitted by the observed width of the absorption line). In the case of the weak ( $v_{\text{lsr}} = -15.4$  km s<sup>-1</sup>) component towards  $\zeta$  Oph, the observed strength of the corresponding Na *D* component (Fig. 2b) provides an additional constraint; the fact that the equivalent width of the *D*<sub>2</sub> line is only 11 times that of  $\lambda 3302$  (*cf.* Tables 2 and 3), whereas the oscillator strength is 70 times larger (Morton 1991), indicates that, in spite of its relative weakness, the *D*<sub>2</sub> line does suffer from significant saturation. Indeed, consideration of the  $\lambda 3302$  and Na *D*<sub>2</sub> curves of growth (allowing for the unresolved hyperfine structure) indicates that this component must have a velocity dispersion  $b \leq 0.15$  km s<sup>-1</sup>, if we consider the  $1\sigma$  equivalent width errors listed in Tables 2 and 3 (although this is relaxed somewhat, to  $b \leq 0.20$  km s<sup>-1</sup>, if we take  $2\sigma$  errors for both lines).

### 3.2 Ca II and Na *D* column density analyses

Column densities and  $b$  values for the three Ca II observations, and the Na *D* observation of  $\zeta$  Oph, were obtained by means of a line profile analysis. Theoretical profiles were generated using DIPS0 (Howarth & Murray 1988), convolved with the instrumental response function, and matched to the observed data. The best-fitting model profiles are superimposed on the observed spectra in Fig. 2, and the values of  $b$  and  $N$  are given in Table 3.

#### 4 COMPARISON WITH PREVIOUS RESULTS

Owing to the difficult spectral region in which they occur (i.e. at wavelengths where the atmospheric transmission is falling off, atmospheric refraction is significant, and optical spectrographs generally have less than optimal efficiency), studies of the  $\lambda$  3302 lines have been performed for relatively few interstellar sightlines. Here we briefly summarize these earlier observations, drawing attention to the sightlines which are common to the present work.

Herbig (1968) observed the  $\lambda$  3302 doublet towards  $\zeta$  Oph; de Boer & Pottasch (1974) presented new data for six stars (including  $\chi$  Oph), and discussed other observations reported in the literature (including previously unpublished results obtained by Herbig); Cohen (1974) presented data for a further six stars; Crutcher (1975a) reported observations towards 21 stars (including  $\omega^1$  Sco,  $\chi$  Oph and  $\zeta$  Oph); Hobbs (1978) presented observations towards 10 stars (including  $\zeta$  Oph); and Chaffee & Dunham (1979) obtained  $\lambda$  3302 data for three stars in the Cep OB2 association.

Table 4 compares the equivalent widths obtained here with those found in the earlier studies for the three stars in common. It will be seen that the agreement is very good in the case of  $\chi$  Oph, but less so for  $\zeta$  Oph and  $\omega^1$  Sco. In the case of  $\zeta$  Oph, the present equivalent widths agree well with those given by Herbig (1968), but are significantly larger than those found by Crutcher (1975a; resolution  $8 \text{ km s}^{-1}$ ) and Hobbs (1978; resolution  $4.6 \text{ km s}^{-1}$ , obtained with a coude scanner rather than the PEPSIOS interferometer). Given the agreement found for  $\chi$  Oph, the disagreement with the results of Crutcher (1975a) and Hobbs (1978) for  $\zeta$  Oph is surprising, the more so as their photoelectric results might be considered more reliable than the photographic data obtained by Herbig (1968). However, apart from the agreement with Herbig's values, there are several reasons for confidence in the present  $\zeta$  Oph results.

(i) Previous comparisons between Mt Stromlo coude spectra and Hobbs' (higher resolution) PEPSIOS observations of the Na D and Ca K lines have generally shown very good agreement (e.g. table 3 of Crawford 1991b). Compare also the total equivalent width ( $40 \pm 2 \text{ m}\text{\AA}$ ) found here for the Ca K line towards  $\zeta$  Oph with the value of  $41 \text{ m}\text{\AA}$  given by Hobbs (1978).

(ii) The higher quality of the present results is illustrated by the clear detection of the weaker ( $v_{\text{lsr}} = -15.4 \text{ km s}^{-1}$ ) component towards  $\zeta$  Oph (Fig. 1f). This component was not detected by Hobbs (1978; cf. his fig. 2b), in spite of the fact that the two spectra appear to have very similar signal-to-noise ratios.

(iii) Crutcher (1975a) states that his scanning method may have underestimated the equivalent widths, although, based on a comparison with the results of de Boer & Pottasch (1974), he infers that this amounts to only about 6 per cent. Note, however, that in the case of  $\omega^1$  Sco, Crutcher's failure to detect the weaker component of the doublet appears to imply an impossible doublet ratio (i.e.  $DR > 2$ ).

(iv) The equivalent widths given by Crutcher (1975a) imply a velocity dispersion of  $b = 0.7 \pm 0.1 \text{ km s}^{-1}$  for the main  $\zeta$  Oph cloud (which is lower than the value actually tabulated by Crutcher because of the effect of hyperfine structure). The present work results in the somewhat higher value of  $0.9^{+0.2}_{-0.1} \text{ km s}^{-1}$  (Table 2), which is in better agreement with the very accurate value ( $0.88 \pm 0.02 \text{ km s}^{-1}$ ) determined by Crane *et al.* (1986) from the CN lines.

As a final comment on the equivalent width discrepancies found for  $\zeta$  Oph, we note that the brightness of this star (which ordinarily makes it so useful for interstellar line studies) increases the possibility of intensity calibration errors. First, there is the danger of stray light reaching the detector, which, if it is not properly allowed for, will cause the equivalent widths to be underestimated; we note that the subtraction of the inter-order background performed as part of the data reduction procedure (Section 2) should have corrected for the effect of any scattered light in the present work. Secondly, there is the possibility of insidious saturation effects occurring with electronic detectors at high photon count rates. For example, the Mt Stromlo PCA is known to become non-linear at photon count rates above about 0.25 Hz per pixel; however, as the  $\lambda$  3302 spectrum of  $\zeta$  Oph described here was obtained with a mean count rate approximately an order of magnitude lower than this (0.028 Hz), we can be confident that the present observations have not suffered from detector saturation.

#### 5 Na I COLUMN DENSITIES AND VELOCITY STRUCTURE

The range of Na I column densities obtained from the  $\lambda$  3302 doublet are compared with those obtained from previous analyses of the Na D lines in Fig. 3. The heavy error bars indicate the range of column densities obtained from the  $\lambda$  3302 analysis

**Table 4.** Comparison between the equivalent widths obtained here and those obtained by earlier authors for three stars in common.

Star	$w_{\lambda}$ ( $\lambda$ 3302.368)					$w_{\lambda}$ ( $\lambda$ 3302.978)				
	Here	Ref (1)	Ref (2)	Ref (3)	Ref (4)	Here	Ref (1)	Ref (2)	Ref (3)	Ref (4)
$\omega^1$ Sco	$10.3 \pm 1.5$	....	....	$3.1 \pm 0.7$	....	$5.2 \pm 1.4$	....	....	$\leq 0.7$	....
$\chi$ Oph	$32.6 \pm 2.0$	....	34	$30.5 \pm 1.2$	....	$25.9 \pm 1.9$	....	24	$24.0 \pm 1.2$	....
$\zeta$ Oph	$31.2 \pm 1.3$	28.7	....	$23.1 \pm 0.6$	24	$24.6 \pm 1.3$	22.3	....	$16.8 \pm 0.6$	19

References: (1) Herbig (1968); (2) de Boer & Pottasch (1974; personal communication from G. H. Herbig); (3) Crutcher (1975a); (4) Hobbs (1978).



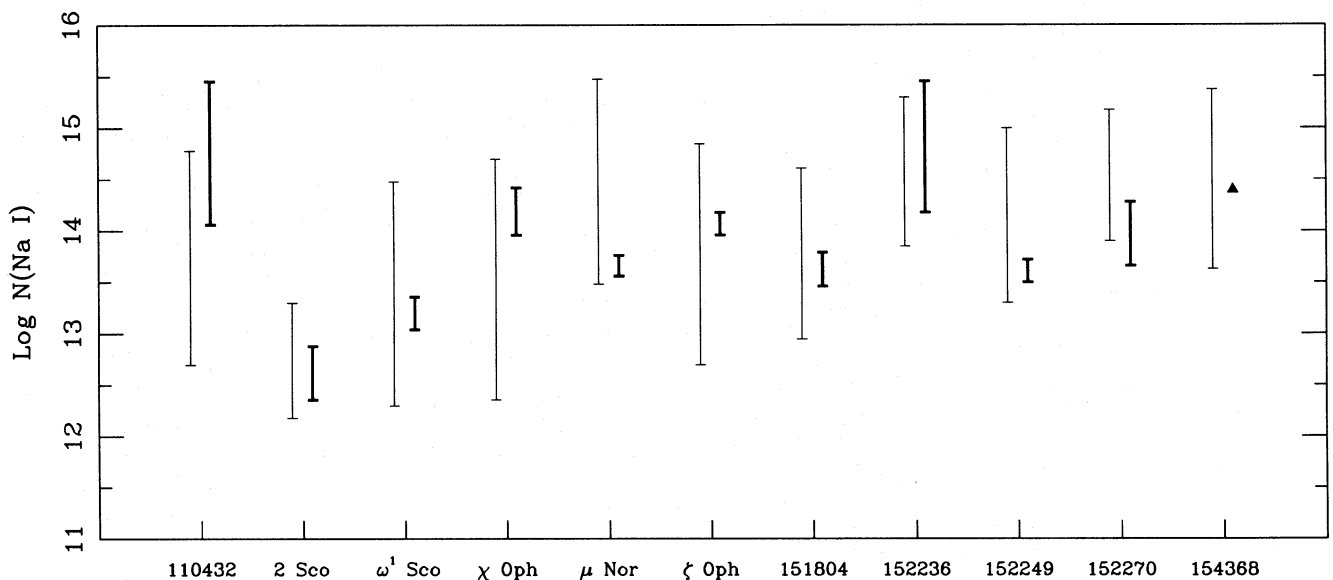


**Figure 3.** Comparison between the Na I column densities obtained from the analysis of the  $\lambda 3302$  doublet (bold error bars) and those obtained from previous studies of the (fully saturated) Na D lines (light error bars; Crawford 1991a, b; Crawford *et al.* 1989). The lower limit found for HD 154368 (*cf.* Table 2) is plotted as an upwards-pointing triangle. Note that, in most cases, the  $\lambda 3302$  analysis has reduced the column density uncertainty by more than an order of magnitude.

towards each star; where more than one velocity component was observed, the column densities of each have been added. The light-weight error bars indicate the maximum range of column density determined from the D lines at the same velocities as the  $\lambda 3302$  absorption (Crawford *et al.* 1989; Crawford 1991a, b). The Na D lines are fully saturated in this velocity range, and this accounts for the very large uncertainties in the column densities derived from them; the upper limits to the D-line column densities in Fig. 3 (mostly in the region  $\log N \sim 15$ ) are constrained by the absence of damping wings in the observed Na D line profiles.

Fig. 3 shows that, as expected, the  $\lambda 3302$  analysis has greatly reduced the Na I column density uncertainties for most of the observed stars. Only in the case of HD 152236 are the Na D and  $\lambda 3302$  uncertainties comparable, due to the fact that three velocity components were observed at the latter wavelength, all of which have poorly constrained column densities (*cf.* Table 2). Fig. 4 compares the velocity structure found in the stronger component of the  $\lambda 3302$  doublet with that found in the interstellar Na D and CH ( $\lambda 4300$ ) lines observed towards the same stars.

For the purposes of more detailed discussion, the stars may naturally be divided into three groups: the single star HD 110432 (located behind the Southern Coalsack); stars in the upper Scorpius subgroup of the Sco–Cen association (2 Sco,  $\omega^1$  Sco,  $\chi$  Oph and  $\zeta$  Oph); and stars in the direction of the Sco OB1 association (four association member stars: HD 151804, 152236, 152249 and 152270; plus two non-members,  $\mu$  Nor and HD 154368, which lie nearby on the sky).

### 5.1 HD 110432

High-resolution observations of interstellar Na I, Ca II, CH and CH<sup>+</sup> towards this star have been reported by Crawford (1991a); observations of interstellar CH, CN and C<sub>2</sub> have been presented by van Dishoeck & Black (1989) and Gredel, van Dishoeck & Black (1991). These observations reveal the presence of a strong component (fully saturated in the case of Na I D) at an LSR velocity of about  $-1.6 \pm 0.5$  km s<sup>-1</sup>, with a weaker component (positively identified only in CH) at a velocity of  $-5.7 \pm 1.5$  km s<sup>-1</sup>. The  $\lambda 3302$  lines observed here ( $v_{\text{lsr}} = -0.5$  km s<sup>-1</sup>) mainly belong to the former component, although the asymmetry in the line profile may be due to Na absorption associated with the weaker CH component to the blue (Fig. 4a). The velocities of both CH components present towards HD 110432 are consistent with those found in the Coalsack CO emission by Nyman Bronfman & Thaddeus (1989).

Based on the assumption of a single velocity component (but allowing for the effect of hyperfine structure), Crawford (1991a) found the Na I column density to lie in the range  $12.70 \leq \log N \leq 14.78$  cm<sup>-2</sup> from an analysis of the saturated D<sub>2</sub> line. The  $\lambda 3302$  observations have constrained the Na column density to lie in the upper end of this range (*cf.* Fig. 3). As the upper limit determined from the  $\lambda 3302$  lines is higher than the maximum value consistent with the D<sub>2</sub> observations, we can combine the two to place quite stringent limits on the Na I column density towards HD 110432; specifically that  $14.06 \leq \log N(\text{Na I}) \leq 14.78$ .

### 5.2 Upper Scorpius

The stars 2 Sco,  $\omega^1$  Sco,  $\chi$  Oph and  $\zeta$  Oph all belong to the upper Scorpius subgroup of the nearby ( $d \leq 200$  pc) Sco–Cen association (e.g. de Geus, de Zeeuw & Lub 1989, and references therein). High-resolution observations of the interstellar Na D<sub>2</sub>

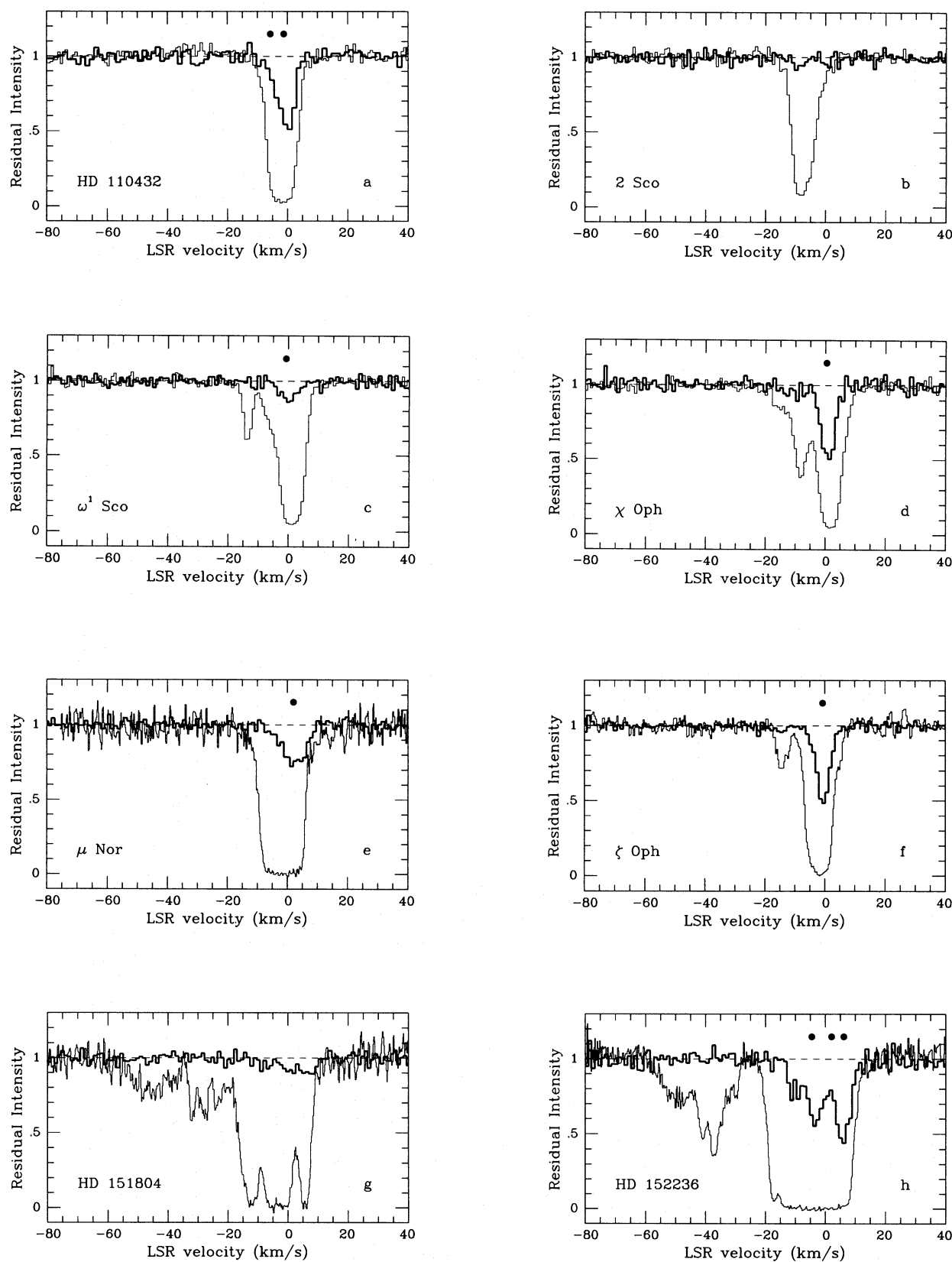


**Figure 4.** Comparison between the velocity structure found in the  $\lambda 3302.368$  and Na I D<sub>2</sub> absorption-line profiles. The  $\lambda 3302$  profiles are drawn with heavy lines, the Na I D<sub>2</sub> profiles with light lines. The velocities of the interstellar CH lines present towards these stars are indicated by filled circles (references are given in the text); it is clear that the  $\lambda 3302$  components arise predominantly in the foreground molecular clouds (but see note 5 Table 2 concerning the spectrum of HD 152270). Note also that the high-velocity Na I components present towards the four Sco OB1 stars (g-j) are not observed at  $\lambda 3302$ , and that additional low-velocity components are required to account for the widths of the saturated Na I absorption troughs towards these stars.

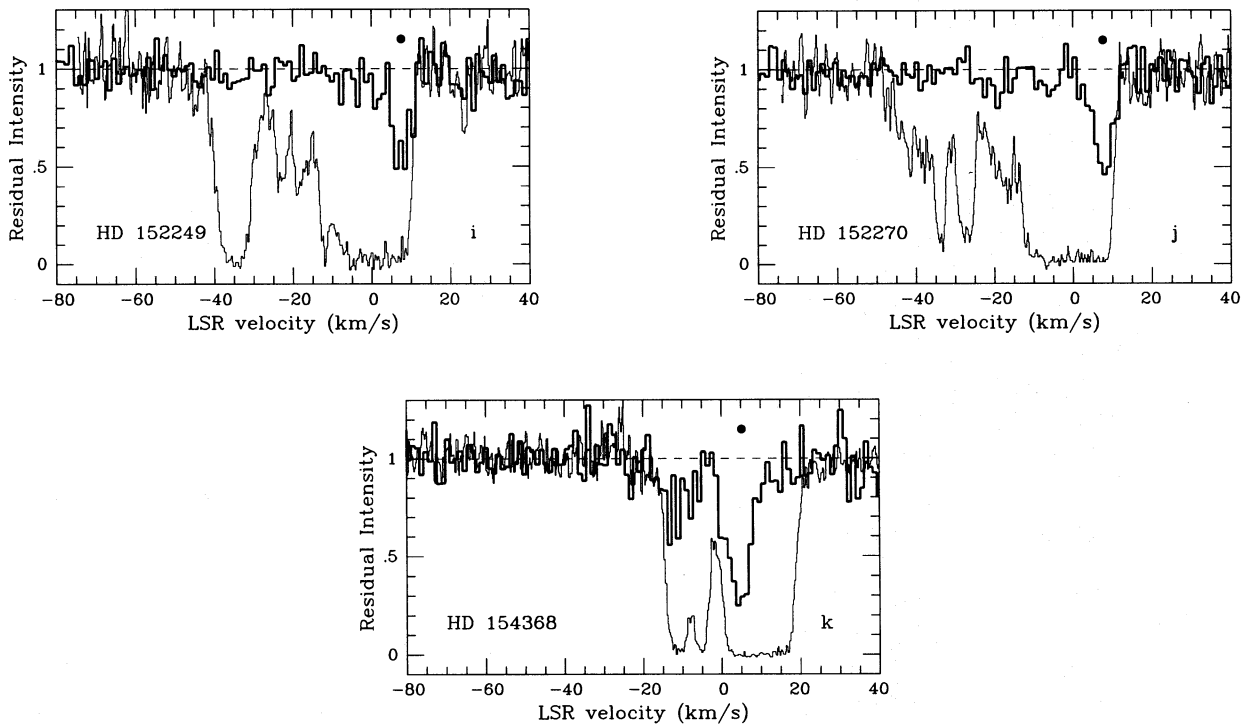


Figure 4 - continued

and Ca II *K* lines towards the first three named stars have been presented in an earlier paper (Crawford 1991b); spectra of Na I and Ca II towards  $\zeta$  Oph are included in this paper (see also Hobbs 1969a, 1974).

The interstellar Na *D* spectra of  $\omega^1$  Sco,  $\chi$  Oph and  $\zeta$  Oph are broadly similar: each has a very strong, fully saturated component within  $\pm 2$  km s $^{-1}$  of zero LSR velocity, and each has additional weaker components to the blue, extending to  $v_{\text{lsr}} \sim -15$  km s $^{-1}$ . The strong, low-velocity components are consistent with an origin in outlying gas associated with the  $\rho$  Oph molecular cloud (*cf.* Dame *et al.* 1987; Crawford 1991b). This suggestion is supported by the observation of molecular lines at these velocities: CH and CH $^+$  towards all three stars (Danks, Federman & Lambert 1984; Lambert & Danks 1986), and CN and C $_2$  towards  $\chi$  Oph and  $\zeta$  Oph (Hobbs & Campbell 1982; van Dishoeck & de Zeeuw 1984). The  $\lambda 3302$  components occur at these velocities (Fig. 4c, d, f), and the column densities given in Table 2 therefore refer to the molecular clouds present towards these stars.

The velocity structure towards 2 Sco is slightly different; the main Na *D* component occurs at a more negative velocity ( $v_{\text{lsr}} = -8.1$  km s $^{-1}$ ; Crawford 1991b), and the  $\lambda 3302$  line is very weak (Fig. 4b). This, together with non-observations of molecules, is consistent with 2 Sco lying in front of the dense clouds responsible for the molecular absorption towards the other upper Scorpius stars (de Geus *et al.* 1989; *cf.* fig. 1a of Crawford 1991b).

### 5.3 The Sco OB1 association

High-resolution observations of the interstellar Na I *D* and Ca II *K* lines towards the stars HD 151804, 152236, 152249 and 152270 (all members of the Sco OB1 association), and Na *D* spectra of  $\mu$  Nor and HD 154368, have been presented by Crawford *et al.* (1989). For completeness, Ca II spectra of the latter two stars are included in the present paper (Fig. 2c, d).

All these stars have very strong, fully saturated interstellar Na *D* lines at low velocities, and in this respect are similar to the other stars discussed above. However, the Sco OB1 stars also exhibit complex blueshifted absorption components [with LSR velocities as negative as  $-55$  km s $^{-1}$ ; interpreted by Crawford *et al.* (1989) as arising in an expanding shell centred on the OB association], and weaker redshifted (mostly Ca II) components with LSR velocities extending up to about  $+20$  km s $^{-1}$ . The complicated Na *D* line profiles towards the four Sco OB1 stars are compared with those of the  $\lambda 3302$  line in Fig. 4(g–j). The velocity structure at  $\lambda 3302$  is much simpler than that observed in the *D* lines, with all the absorption found to occur at low LSR velocities. Indeed, it is apparent from Fig. 4 that the  $\lambda 3302$  components all occur towards the positive-velocity edge of the saturated Na *D* troughs, and that (with the possible exception of those towards HD 152236) they are insufficient to account for the total velocity extent of these features. This indicates that additional, low-velocity components must be present; although saturated in Na *D*, these additional components have insufficient Na I column densities ( $\log N \lesssim 13$ ) for the  $\lambda 3302$  lines to be observable in the present spectra.

Lines due to interstellar CH (with associated CH $^+$ ) were found towards three of the four Sco OB1 stars by Crawford (1989), and the velocities of these are indicated in Fig. 4 (note that, owing to the failure to record a Th–Ar spectrum for the HD 152270

exposure, the velocity of the  $\lambda$  3302 line towards this star was tied to that of the CH line; the agreement between the velocities of these species for the other stars confirms that this procedure was reasonable under the circumstances). Interstellar CN is present at the velocities of the CH lines towards HD 152236 (two out of three components), HD 152249, and HD 152270 (Crawford 1990). The Na I column densities obtained at these velocities from the  $\lambda$  3302 analysis (Table 2) therefore pertain to the molecular clouds in the line of sight. As discussed by Crawford (1992), these molecular components (excluding the most negative-velocity CH component towards HD 152236) probably arise in outlying gas associated with the Lupus molecular cloud complex. Molecules have also been observed at the velocity of the  $\lambda$  3302 component towards  $\mu$  Nor (CH and CH<sup>+</sup>; Danks *et al.* 1984; Lambert & Danks 1986), and at the velocity of the stronger of the two  $\lambda$  3302 components towards HD 154368 (CH, CN, C<sub>2</sub>; van Dishoeck & Black 1989).

Interstellar CH was not detected towards HD 151804 by Crawford (1989), and we note that this is consistent with the observation that the  $\lambda$  3302 lines are much weaker towards this star than towards the other Sco OB1 stars studied here. There is a CH<sup>+</sup> line at  $v_{\text{lsr}} = +0.4$  km s<sup>-1</sup>, which may perhaps be identified with the bluer of the two  $\lambda$  3302 components. We note in passing that these observations have some bearing on the discrepancy between the CH observations towards this star reported by Crawford (1989) and Danks *et al.* (1984); briefly, Danks *et al.* reported weak CH components at LSR velocities +9.2 and +11.8 km s<sup>-1</sup>, which were not observed by Crawford (1989), and we point out that these velocities do not agree with those of the  $\lambda$  3302 components, where molecular lines would be most expected.

The  $\lambda$  3302 lines were not detected at the velocities of the Sco OB1 shell components, and the equivalent-width upper limits at these velocities are consistent with the column densities derived from the Na D lines (i.e.  $\log N_{\text{Na I}} \lesssim 12$ , *cf.* table 4 of Crawford *et al.* 1989). It is worth drawing special attention to the  $v_{\text{lsr}} = -34$  km s<sup>-1</sup> Na D component found towards HD 152249 (Fig. 4i). This component is unusual among the Sco OB1 high-velocity components because its core reaches zero residual intensity, a circumstance that makes its column density very uncertain; Crawford *et al.* (1989) obtained a range of  $12.48 \leq \log N \leq 14.90$ . In the earlier paper it was argued that the true value probably lies at the lower end of this range, as this would give it a Na I/Ca II ratio comparable to those of the other high-velocity components. The fact that this component was not detected at  $\lambda$  3302 shows that this suggestion was correct. The equivalent-width upper limit at this velocity (6.4 mÅ) implies that  $\log N \leq 12.92$ ; this results in a new upper limit to  $\log(\text{Na I/Ca II})$  of 1.04, which brings this component into line with all the others (*cf.* fig. 7 of Crawford *et al.* 1989).

## 6 THE Na I/Ca II RATIOS

A major aim of the present study was to obtain accurate values for the Na I/Ca II column density ratios in the dense, low-velocity gas known to exist towards these stars from the presence of very strong Na D and molecular lines. Owing to the heavy saturation in the D lines, Na I/Ca II ratios obtained from them are typically uncertain by about two orders of magnitude (*cf.* fig. 7 of Crawford *et al.* 1989). Na I/Ca II ratios for the (generally less saturated) high-velocity components are much better constrained. Previous work (Routly & Spitzer 1952; Siluk & Silk 1974; Crawford *et al.* 1989) has clearly demonstrated that the Na I/Ca II ratios are higher in low-velocity material (the ‘Routly–Spitzer’ effect), but the large uncertainties arising from line saturation have made it difficult to quantify the magnitude of this effect.

The Na I/Ca II column density ratios obtained for the Na I components identified at  $\lambda$  3302 are listed in Table 5. These ratios are primarily based on the Na I column densities obtained from the  $\lambda$  3302 analysis (Table 2), but additional constraints provided by earlier observations (in particular, the absence of damping wings in the  $D_2$  line profiles) have been employed wherever possible. References to the Ca II observations used for the determination of the Na I/Ca II ratios are also given in the table.

Fig. 5 shows the Na I/Ca II ratios for all the velocity components identified towards the 11 stars discussed in this paper. The ratios obtained for the components observed in the  $\lambda$  3302 doublet (i.e. those listed in Table 5) are indicated by bold error bars. The ratios for components that were not observable at  $\lambda$  3302 have been obtained from the previous analyses of the Na D lines towards these stars (Crawford *et al.* 1989; Crawford 1991b), and are indicated by light-weight error bars. As discussed in Section 5.3 (and clearly illustrated in Fig. 4), the  $\lambda$  3302 components are unable to account for all the low-velocity, fully saturated Na D absorption found towards the Sco OB1 stars, which implies the presence of additional, low-velocity components with  $\log N(\text{Na I}) \lesssim 13.0$ . Although this velocity range was found to be fully saturated in the Na D lines, Crawford *et al.* (1989) found clear evidence for discrete Ca II absorption components, and the Na I/Ca II ratios of these (based on a re-analysis of the Na D data, allowing for the upper limits implied by the non-detection of the  $\lambda$  3302 lines) are included in Fig. 5.

We now turn to a detailed discussion of the different types of component present in Fig. 5.

### 6.1 Components observed at $\lambda$ 3302

A total of 16  $\lambda$  3302 components was detected towards the 11 stars discussed in this paper. All of these components (except possibly the +6.7 km s<sup>-1</sup> component towards HD 151804) have Na I/Ca II ratios greater than 10, and some may have ratios as high as 10<sup>3</sup>. All these components have low LSR velocities ( $-15 \lesssim v_{\text{lsr}} \lesssim +10$  km s<sup>-1</sup>), and eight of the 16 occur in the very restricted range  $|v_{\text{lsr}}| < 5$  km s<sup>-1</sup>. This is as expected from the Routly–Spitzer effect, but the ratios at the upper end of the observed range are greater than those generally quoted for low-velocity clouds. For example, the present analysis of the main component towards  $\zeta$  Oph yields a Na I/Ca II ratio of  $310^{+140}_{-110}$  [which is consistent with the value of 280 obtained by Crutcher (1975b) from a study of the D lines, but much larger than the much-quoted value of 90 listed by Siluk & Silk (1974)]; the main components towards HD 110432,  $\chi$  Oph, and HD 152236 also have Na I/Ca II ratios that are constrained to be in excess of 10<sup>2</sup>.

We can examine the implications of these high Na I/Ca II ratios by considering the ionization balance [similar calculations have been presented by Seaton (1951), Hobbs (1976) and Jura (1976), but we take the opportunity here to employ updated



**Table 5.** Na I/Ca II ratios for the components observed at 3302 Å. These ratios are based on the  $\lambda 3302$  analysis, unless otherwise noted. The velocities of the associated Ca II components are given so that these may be located in the references given; the Ca II profiles towards the Sco OB1 stars are very complicated (Crawford *et al.* 1989), and the velocities of individual components towards these stars are probably uncertain by about  $\pm 2$  km s $^{-1}$ .

Star	$v_{lsr}(\lambda 3302)$ (km s $^{-1}$ )	$v_{lsr}(\text{Ca II})$ (km s $^{-1}$ )	Ref	Log (Na I/Ca II)	Notes
110432	-0.5	-1.4	1	$2.35^{+0.58}_{-0.33}$	a
2 Sco	-9.0	-8.1	2	$1.76^{+0.42}_{-0.40}$	
$\omega^1$ Sco	-0.4	+1.1	2	$1.50^{+0.32}_{-0.11}$	
$\chi$ Oph	+0.6	+0.8	2	$2.31^{+0.37}_{-0.25}$	
$\mu$ Nor	+2.1	0, +7	3	$1.08^{+0.20}_{-0.12}$	b
$\zeta$ Oph	-15.4	-14.3	3	$1.52^{+0.44}_{-0.16}$	
	-0.7	-0.5	3	$2.49^{+0.16}_{-0.18}$	
151804	-0.8	-2.8	4	$1.09^{+0.08}_{-0.11}$	
	+6.7	+5.6	4	$0.90^{+0.51}_{-0.28}$	
152236	-10.1	-11.2	4	$2.08^{+0.88}_{-0.88}$	a
	-3.0	-1.9	4	$1.36^{+1.46}_{-0.38}$	
	+6.1	+6.8	4	$2.50^{+0.80}_{-0.24}$	
152249	+7.5	+5.5	4	$1.71^{+0.20}_{-0.11}$	
152270	+7.7	+6.0	4	$1.99^{+0.46}_{-0.25}$	
154368	-11.7	-13.0	3	$1.93^{+0.85}_{-0.38}$	a
	+4.3	+3.6	3	$1.97^{+0.63}_{-0.63}$	a

References for Ca II observations: (1) Crawford (1991a); (2) Crawford (1991b); (3) this work; (4) Crawford *et al.* (1989).

Notes: (a) Upper limit set by observations of the interstellar Na  $D_2$  line in these components (Crawford 1991a; Crawford *et al.* 1989). (b) Two Ca II components lie within the velocity range occupied by the  $\lambda 3302$  lines; the column densities of these have been added.

photoionization and recombination rates, and to allow for the effect of shielding by the clouds]. Under interstellar conditions, the total column densities of Na and Ca are given by

$$N(\text{Na}) = N(\text{Na}^0) + N(\text{Na}^+) \quad (3)$$

and

$$N(\text{Ca}) = N(\text{Ca}^0) + N(\text{Ca}^+) + N(\text{Ca}^{++}). \quad (4)$$

If it is assumed that the ratios  $N(\text{Na}^0)/N(\text{Na}^+)$ ,  $N(\text{Ca}^0)/N(\text{Ca}^+)$  and  $N(\text{Ca}^+)/N(\text{Ca}^{++})$  are maintained by a balance between photoionization and radiative recombination, equations (3) and (4) can be rearranged to give the Na I/Ca II ratio as a function of the (gas-phase) Na/Ca abundance ratio:

$$\frac{N(\text{Na I})}{N(\text{Ca II})} = \frac{N(\text{Na})}{N(\text{Ca})} \frac{\{\alpha(\text{Ca}^0)n_e/\Gamma(\text{Ca}^0)\} + 1 + \{\Gamma(\text{Ca}^+)/\alpha(\text{Ca}^+)n_e\}}{\{1 + [\Gamma(\text{Na}^0)/\alpha(\text{Na}^0)n_e]\}}. \quad (5)$$

Here,  $\Gamma(\text{Na}^0)$  is the photoionization rate (s $^{-1}$ ) of Na $^0$  and  $\alpha(\text{Na}^0)$  is the recombination rate (cm $^3$  s $^{-1}$ ) for Na $^+$  to Na $^0$ , and similarly for the other ions;  $n_e$  is the electron density (cm $^{-3}$ ). The recombination rates are temperature dependent, and the photoionization rates are dependent on the intensity of the interstellar radiation field (and hence on the degree of shielding provided by the cloud).



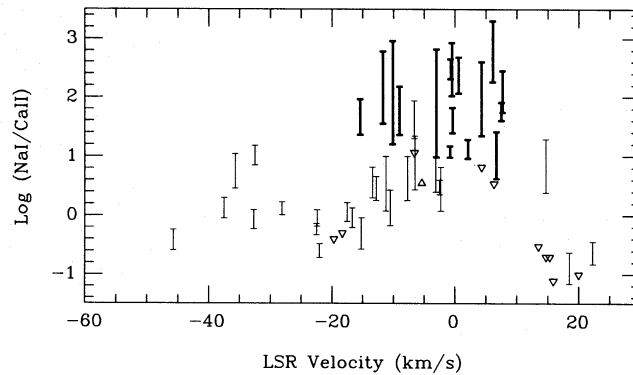


**Figure 5.** The Na I/Ca II ratios of all the velocity components known to be present towards these stars. The ratios determined from the  $\lambda$  3302 lines are indicated by bold error bars. The others come from previous work (Crawford *et al.* 1989; Crawford 1991b). See text for discussion.

Electron densities and temperatures for the clouds towards  $\zeta$  Oph and HD 154368 (together with other representative diffuse molecular clouds) have been listed by Black & van Dishoeck (1991). Based on these values, we will assume a temperature of 30 K for the recombination rates, which we take from the tabulations of Shull & Van Steenberg (1982; Ca<sup>0</sup>, Ca<sup>+</sup>) and Aldrovandi & Péquignot (1974; Na<sup>0</sup>). We take the photoionization rates from van Dishoeck (1988; *cf.* her table 3). Given these values, equation (5) reduces to

$$\frac{N(\text{Na I})}{N(\text{Ca II})} = \frac{N(\text{Na})}{N(\text{Ca})} \frac{[0.0614 \exp(+1.68 A_V) n_e^2 + n_e + 0.0325 \exp(-3.33 A_V)]}{[n_e + 1.23 \exp(-1.78 A_V)]}, \quad (6)$$

where  $A_V$  is the visual extinction to the point within the cloud where photoionization occurs. At low electron densities ( $n_e \lesssim 0.1 \text{ cm}^{-3}$ ) the first term in the numerator (which gives the Ca<sup>0</sup> contribution to the total Ca abundance) is usually negligible, although it can become significant for large values of  $A_V$ .

For  $A_V = 0.4$  mag (appropriate for the extinction to the centre of the  $\zeta$  Oph cloud), and  $n_e = 0.1 \text{ cm}^{-3}$  (which is within a factor of 2 of most of the electron densities listed by Black & van Dishoeck 1991), we obtain

$$\frac{N(\text{Na I})}{N(\text{Ca II})} \approx 0.16 \frac{N(\text{Na})}{N(\text{Ca})}. \quad (7)$$

The factor 0.16 in equation (7) changes by less than plus or minus a factor 2 (i.e. takes values between 0.07 and 0.34) for values of  $n_e$  in the range  $0.05\text{--}0.2 \text{ cm}^{-3}$ , and values of  $A_V$  in the range  $0.0\text{--}0.6$  mag.

Equation (7) indicates that a Na I/Ca II ratio of 300 (such as that found towards  $\zeta$  Oph, and which is consistent also with ratios determined for the main components towards HD 110432,  $\chi$  Oph and HD 152236) implies that there are approximately 2000 times as many Na as Ca atoms present in the gas phase. As Na and Ca have approximately equal cosmic abundances (Grevesse 1984), this indicates substantial differential depletion of calcium, an inference originally made by Howard, Wentzel & McGee (1963; see also Herbig 1968; Jura 1976). The degree to which elements are depleted in the interstellar gas is usually indicated by the logarithmic depletion factors,  $\delta_x$ , where

$$\delta_x = \log[N(\text{X})/N(\text{H})] - \log[N(\text{X})/N(\text{H})]_{\odot}. \quad (8)$$

Adopting the solar abundances given by Grevesse (1984), we can express the (gas phase) Na/Ca ratio in terms of the depletion factors as follows:

$$\delta_{\text{Ca}} = \delta_{\text{Na}} - \log(\text{Na/Ca}) - 0.03. \quad (9)$$

The gas-phase Na/Ca ratio can be estimated from the Na I/Ca II ratio using equation (7). Sodium is generally lightly depleted in the diffuse interstellar medium ( $\delta_{\text{Na}} \gtrsim -1$ ; e.g. Jura 1975; Phillips, Pettini & Gondhalekar 1984); Phillips *et al.* (1984) found an average value of  $\delta_{\text{Na}} \approx -0.6$  over a large range of cloud densities. If we adopt this value in equation (9) we obtain  $\delta_{\text{Ca}} \approx -3.9$  for Na I/Ca II = 300. More generally, we find that  $\delta_{\text{Ca}} \leq -3.4$  for Na I/Ca II  $\geq 100$ .

Most of these components are associated with interstellar molecules (Fig. 4), which indicates that they arise in physically dense clouds, rather than in long lines of sight through less dense material. In fact, four of the clouds observed at  $\lambda$  3302 have had their densities measured from an analysis of the rotational excitation of the C<sub>2</sub> molecule. These densities [ $n \equiv n(\text{H}) + n(\text{H}_2)$ ] are as follows: HD 110432,  $n \lesssim 200 \text{ cm}^{-3}$  (van Dishoeck & Black 1989);  $\chi$  Oph,  $n \approx 150\text{--}175 \text{ cm}^{-3}$  (van Dishoeck & de Zeeuw 1984);  $\zeta$  Oph (main component),  $n \approx 100\text{--}200 \text{ cm}^{-3}$  (van Dishoeck & Black 1986a); and HD 154368 (main component),  $n \approx 200\text{--}255 \text{ cm}^{-3}$  (van Dishoeck & de Zeeuw 1984).

Significant Ca depletions (and thus large Na I/Ca II ratios) are expected in dense clouds owing to the adsorption of gas-phase Ca atoms on to the surfaces of interstellar grains. As Ca has a much greater adsorption binding energy than Na (Barlow 1978), differential depletion is expected, and empirical evidence for it has been obtained by Phillips *et al.* (1984; and, for other

elements, by Phillips, Gondhalekar & Pettini 1982; Jenkins, Savage & Spitzer 1986). On the basis of the present results, we can quantify this effect to the extent of stating that densities of  $n \gtrsim 10^2 \text{ cm}^{-3}$  are sufficient to result in calcium depletions of  $\delta_{\text{Ca}} \approx -4$ .

## 6.2 Low-velocity components not observed at $\lambda 3302$

Although the Na I/Ca II ratios shown in Fig. 5 are broadly consistent with expectations based on the Routly–Spitzer effect (i.e. higher ratios at low absolute velocities), it is clear that there are low-velocity components ( $|v_{\text{lsr}}| \lesssim 10 \text{ km s}^{-1}$ ) with significantly lower Na I/Ca II ratios than those of the denser (molecular) clouds discussed above. These components have Na I/Ca II ratios in the range 2–10 (*cf.* Fig. 5), and values of this order were identified by Hobbs (1976) to be typical or diffuse (non-molecular) clouds characterized by  $n_{\text{H}} \sim 10 \text{ cm}^{-3}$  and  $T \sim 100 \text{ K}$ . In order to calculate the calcium depletions it is necessary to estimate the electron density, which has not been directly measured for these components. Kulkarni & Heiles (1987) have given the following expression for the electron density in diffuse clouds:

$$n_e = n_i + \frac{n_i}{2} \left[ \left( 1 + \frac{4 \zeta_{\text{cr}} n_{\text{H}}}{\alpha n_i^2} \right)^{1/2} - 1 \right], \quad (10)$$

where  $n_i$  is the number density of metallic ions (dominantly carbon),  $\zeta_{\text{cr}}$  is the cosmic ray ionization rate, and  $\alpha$  is the hydrogen recombination coefficient. If we assume a 50 per cent depletion of carbon (i.e.  $n_i/n_{\text{H}} \sim 2 \times 10^{-4}$ ),  $\alpha = 4 \times 10^{-13} (T/6000 \text{ K})^{-1/2} \text{ cm}^3 \text{ s}^{-1}$  (Kulkarni & Heiles 1987) and  $\zeta_{\text{cr}} = 5 \times 10^{-17} \text{ s}^{-1}$  (adopted by van Dishoeck & Black 1986b), equation (10) gives  $n_e = 0.014 \text{ cm}^{-3}$  for  $n_{\text{H}} = 10 \text{ cm}^{-3}$ . Using this value of  $n_e$ , and adopting  $A_V = 0$  and  $T = 100 \text{ K}$ , the numerical factor in equation (7) takes the value 0.036. This implies that, for Na I/Ca II = 4 and  $T = 100 \text{ K}$ ,  $\delta_{\text{Ca}} = -2.7$  if  $\delta_{\text{Na}} = -0.6$  (or  $\delta_{\text{Ca}} = -2.1$  if Na is undepleted). Thus the lower Na I/Ca II ratios of these components reflect a reduced calcium depletion, consistent with the expectation of density-dependent adsorption on to grain surfaces (e.g. Barlow 1978).

## 6.3 The high-velocity components

At high negative and positive velocities ( $v_{\text{lsr}} \lesssim -15 \text{ km s}^{-1}$  and  $\gtrsim +10 \text{ km s}^{-1}$ ) the Na I/Ca II ratios are observed to mostly lie in the range 0.1–1, with the positive-velocity components having values at the lower end of this range. Most of these components are observed towards the Sco OB1 stars, and have been discussed in detail by Crawford *et al.* (1989). Briefly, the high negative velocity components are interpreted as arising in an expanding shell centred on the Sco OB1 association, while the positive-velocity components are attributed to an origin in warm, low-density ‘intercloud’ medium (the absorption of which is masked at lower velocities by the very strong lines arising from the low-velocity diffuse molecular clouds).

Crawford *et al.* (1989) attributed the relatively low Na I/Ca II ratios in the shell components to be due to the removal of adsorbed Ca atoms from the grain surfaces by interstellar shock waves. The very low Na I/Ca II ratios of the positive-velocity (‘intercloud-type’) components indicate that this material has even lower (but probably still non-zero) Ca depletion. A number of studies (e.g. Hobbs 1976; Ferlet, Vidal-Madjar & Gry 1985; Centurion & Vladilo 1991) have concluded that this material has a temperature of several thousand degrees, and an electron density of  $n_e \sim 0.04 \text{ cm}^{-3}$ . Adopting this electron density, and a temperature of  $T = 5000 \text{ K}$ , the numerical factor in equation (7) also takes the value 0.036 (coincidentally the same as that found in Section 6.2 for much cooler gas). If Na retains its approximately constant depletion ( $\delta_{\text{Na}} \approx -0.6$ ) in these components, this implies  $\delta_{\text{Ca}} \approx -1.1$  for Na I/Ca II = 0.1 (or  $\delta_{\text{Ca}} \approx -0.5$  if Na is undepleted). We note, however, that for  $T \gtrsim 7000 \text{ K}$  collisional ionization of  $\text{Na}^0$  leads to a sharp reduction in the Na I/Ca II ratio appropriate for a given value of  $\delta_{\text{Ca}}$  (Pottasch 1972). Thus, if the temperature is above this critical value in these components, Ca may actually be more depleted than indicated above.

Finally, we note that under these conditions ( $A_V = 0$ ,  $n_e = 0.04 \text{ cm}^{-3}$ ,  $T = 5000 \text{ K}$ ), completely undepleted gas ( $\delta_{\text{Na}} = 0$ ,  $\delta_{\text{Ca}} = 0$ ) implies Na I/Ca II = 0.034 [or  $\log(\text{Na I/Ca II}) = -1.5$ ]. Thus, provided that collisional ionization of  $\text{Na}^0$  is unimportant, those components with the most stringent upper limits in Fig. 5 (especially the  $+15.9 \text{ km s}^{-1}$  component towards  $\mu \text{ Nor}$  and the  $+20 \text{ km s}^{-1}$  component towards HD 151804) may arise in essentially undepleted gas.

## 7 CONCLUSIONS

The main conclusions of this paper are as follows.

- (1) Analysis of the  $\lambda 3302$  doublet towards 11 southern stars has resulted in much more accurate Na I column densities (and hence Na I/Ca II ratios) than those obtained from previous studies of the (fully saturated) Na D lines towards these stars (Table 2; Fig. 3).
- (2) The components observed at  $\lambda 3302$  all occur at low LSR velocities ( $-15 \lesssim v_{\text{lsr}} \lesssim +10 \text{ km s}^{-1}$ ), and are generally coincident with components previously identified in molecular lines. In these cases, the resulting Na I column densities pertain to the diffuse molecular cloud(s) present towards these stars. The Na D and Ca K profiles towards many of these indicate the presence of additional (lower density) clouds which are not observed either at  $\lambda 3302$  or in the molecular lines.
- (3) The components identified at  $\lambda 3302$  all have large Na I/Ca II ratios ( $\gtrsim 10$ ); for the  $\lambda 3302$  components present towards HD 110432 and  $\chi \text{ Oph}$ , and the main components towards  $\zeta \text{ Oph}$  and HD 152236, the ratio definitely exceeds  $10^2$  (*cf.* Fig. 5). For the temperatures and electron densities appropriate for these diffuse molecular clouds (e.g. Black & van Dishoeck 1991), Na I/Ca II  $\gtrsim 10^2$  implies a calcium depletion of  $\delta_{\text{Ca}} \lesssim -3.4$ . In the particular case of the main  $\zeta \text{ Oph}$  cloud (Na I/Ca II =  $310 \pm 140$ ), we find  $\delta_{\text{Ca}} \sim -3.9$ . Based on independent estimates of the cloud densities, we conclude that this degree of Ca depletion results from Ca adsorption on to grain surfaces in clouds having  $n_{\text{H}} \gtrsim 10^2 \text{ cm}^{-3}$ .

(4) The lower Na I/Ca II ratios ( $\approx 4$ ) of the additional low-velocity components (i.e. those *not* observed in the  $\lambda$  3302 lines) imply that Ca is approximately an order of magnitude *less* depleted in these clouds ( $\delta_{\text{Ca}} \approx -2.7$ ) than in the molecular clouds which are present towards many of the same stars. This is consistent with reduced Ca atom adsorption on to grain surfaces in lower density clouds.

(5) Quantitative analysis of the Na I/Ca II ratios of the high-velocity components present towards the Sco OB1 association (discussed by Crawford *et al.* 1989) indicates that Ca still has a significant depletion ( $\delta_{\text{Ca}} \approx -1$ ) in the negative-velocity ('shell') components, but may approach cosmic abundance in several of the 'intercloud'-type components found at positive LSR velocities.

## ACKNOWLEDGMENTS

I thank the Director of the Mt Stromlo and Siding Spring Observatories for the award of observing time on the 74-inch telescope, and the SERC for financial support. I am grateful to Drs M. J. Barlow and J. C. Blades for permission to reproduce their unpublished Na I spectrum of  $\zeta$  Oph. I thank Mike Barlow, and the referee (Dr L. M. Hobbs), for thoughtful comments on the original manuscript.

## REFERENCES

- Aldrovandi, S. M. V. & Péquignot, D., 1974. *Rev. Brasil. de Fisica*, **4**, 491.  
 Barlow, M. J., 1978. *Mon. Not. R. astr. Soc.*, **183**, 417.  
 Black, J. H. & van Dishoeck, E. F., 1991. *Astrophys. J. Lett.*, **369**, L9.  
 Centurion, M. & Vladilo, G., 1991. *Astrophys. J.*, **372**, 494.  
 Chaffee, F. H. & Dunham, T., 1979. *Astrophys. J.*, **233**, 568.  
 Codina, S. J., de Freitas Pacheco, J. E., Lopes, D. F. & Gilra, D., 1984. *Astr. Astrophys. Suppl.*, **57**, 239.  
 Cohen, J. G., 1974. *Astrophys. J.*, **192**, 379.  
 Crane, P., Hegyi, D. J., Mandolesi, N. & Danks, A. C., 1986. *Astrophys. J.*, **309**, 822.  
 Crawford, I. A., 1989. *Mon. Not. R. astr. Soc.*, **241**, 575.  
 Crawford, I. A., 1990. *Mon. Not. R. astr. Soc.*, **244**, 646.  
 Crawford, I. A., 1991a. *Astr. Astrophys.*, **246**, 210.  
 Crawford, I. A., 1991b. *Astr. Astrophys.*, **247**, 183.  
 Crawford, I. A., 1992. *Mon. Not. R. astr. Soc.*, **254**, 264 (Corrigendum, **257**, 368).  
 Crawford, I. A., Barlow, M. J. & Blades, J. C., 1989. *Astrophys. J.*, **336**, 212.  
 Crutcher, R. M., 1975a. *Astrophys. J.*, **202**, 634.  
 Crutcher, R. M., 1975b. *Astrophys. J.*, **200**, 625.  
 Dame, T. M., Ungerechts, H., Cohen, R. S., de Geus, E. J., Grenier, I. A., May, J., Murphy, D. C., Nyman, L.-Å. & Thaddeus, P., 1987. *Astrophys. J.*, **322**, 706.  
 Danks, A. C., Federman, S. R. & Lambert, D. L., 1984. *Astr. Astrophys.*, **130**, 62.  
 de Boer, K. S. & Pottasch, S. R., 1974. *Astr. Astrophys.*, **32**, 1.  
 de Geus, E. J., de Zeeuw, P. T. & Lub, J., 1989. *Astr. Astrophys.*, **216**, 44.  
 Deutschman, W. A., Davis, R. J. & Schild, R. E., 1976. *Astrophys. J. Suppl.*, **30**, 97.  
 Ferlet, R., Vidal-Madjar, A. & Gry, C., 1985. *Astrophys. J.*, **298**, 838.  
 Gredel, R., van Dishoeck, E. F. & Black, J. H., 1991. *Astr. Astrophys.*, **251**, 625.  
 Grevesse, N., 1984. *Phys. Scripta*, **T 8**, 49.  
 Herbig, G. H., 1968. *Z. Astrophys.*, **68**, 243.  
 Hobbs, L. M., 1969a. *Astrophys. J.*, **157**, 135.  
 Hobbs, L. M., 1969b. *Astrophys. J.*, **157**, 165.  
 Hobbs, L. M., 1974. *Astrophys. J.*, **191**, 381.  
 Hobbs, L. M., 1976. *Astrophys. J. Lett.*, **206**, L117.  
 Hobbs, L. M., 1978. *Astrophys. J. Suppl.*, **38**, 129.  
 Hobbs, L. M. & Campbell, B., 1982. *Astrophys. J.*, **254**, 108.  
 Hobbs, L. M. & Welty, D. E., 1991. *Astrophys. J.*, **368**, 426.  
 Hoffleit, D. & Jaschek, C., 1982. *Bright Star Catalogue*, 4th edn, Yale University Observatory, New Haven.  
 Howard, W. E., Wentzel, D. G. & McGee, R. X., 1963. *Astrophys. J.*, **138**, 988.  
 Howarth, I. D. & Murray, J., 1988. *Starlink User Note*, No. 50.  
 Humphreys, R. M., 1978. *Astrophys. J. Suppl.*, **38**, 309.  
 Jenkins, E. B., Savage, B. D. & Spitzer, L., 1986. *Astrophys. J.*, **301**, 355.  
 Jura, M., 1975. *Astrophys. J.*, **200**, 415.  
 Jura, M., 1976. *Astrophys. J.*, **206**, 691.  
 Kulkarni, S. R. & Heiles, C., 1987. In: *Interstellar Processes*, p. 87, eds Hollenbach, D. J. & Thronson, H. A., Reidel, Dordrecht.  
 Lambert, D. L. & Danks, A. C., 1986. *Astrophys. J.*, **303**, 401.  
 McNutt, D. P. & Mack, J. E., 1963. *J. geophys. Res.*, **68**, 3419.  
 Morton, D. C., 1975. *Astrophys. J.*, **197**, 85.  
 Morton, D. C., 1991. *Astrophys. J. Suppl.*, **77**, 119.  
 Nachman, P. & Hobbs, L. M., 1973. *Astrophys. J.*, **182**, 481.  
 Nyman, L.-Å., Bronfman, L. & Thaddeus, P., 1989. *Astr. Astrophys.*, **216**, 185.

- Phillips, A. P., Gondhalekar, P. M. & Pettini, M., 1982. *Mon. Not. R. astr. Soc.*, **200**, 687.  
Phillips, A. P., Pettini, M. & Gondhalekar, P. M., 1984. *Mon. Not. R. astr. Soc.*, **206**, 337.  
Pottasch, S. R., 1972. *Astr. Astrophys.*, **20**, 245.  
Prinja, R. K., Barlow, M. J. & Howarth, I. D., 1990. *Astrophys. J.*, **361**, 607.  
Rodgers, A. W., Van Harmelen, J., King, D., Conroy, P. & Harding, P., 1988. *Publs astr. Soc. Pacif.*, **100**, 841.  
Routly, P. M. & Spitzer, L., 1952. *Astrophys. J.*, **115**, 227.  
Schild, R. E., Garrison, R. F. & Hiltner, W. A., 1983. *Astrophys. J. Suppl.*, **51**, 321.  
Seaton, M. J., 1951. *Mon. Not. R. astr. Soc.*, **111**, 368.  
Shortridge, K., 1988. *Starlink User Note*, No. 86.  
Shull, J. M. & Van Steenberg, M. E., 1982. *Astrophys. J. Suppl.*, **48**, 95.  
Siluk, R. S. & Silk, J., 1974. *Astrophys. J.*, **192**, 51.  
Somerville, W. B., 1988. *Observatory*, **108**, 44.  
Strömgren, B., 1948. *Astrophys. J.*, **108**, 242.  
van Dishoeck, E. F., 1988. In: *Rate Coefficients in Astrochemistry*, p. 49, eds Millar, T. J. & Williams, D. A., Kluwer Academic Publishers, Dordrecht.  
van Dishoeck, E. F. & de Zeeuw, T., 1984. *Mon. Not. R. astr. Soc.*, **206**, 383.  
van Dishoeck, E. F. & Black, J. H., 1986a. *Astrophys. J.*, **307**, 332.  
van Dishoeck, E. F. & Black, J. H., 1986b. *Astrophys. J. Suppl.*, **62**, 109.  
van Dishoeck, E. F. & Black, J. H., 1989. *Astrophys. J.*, **340**, 273.  
van Genderen, A. M., Bijleveld, W. & van Groningen, E., 1984. *Astr. Astrophys. Suppl.*, **58**, 537.